

# Transport properties of solid-electrolyte layers in lithium iodine batteries

E.S. Nimon \*, A.V. Shirokov, N.P. Kovynev, A.L. Lvov, I.A. Pridatko

*Saratov State University, Scientific Research Institute of Chemistry, Astrakhanskaya 83, Saratov 410026, Russian Federation*

Received 15 August 1994; in revised form 23 December 1994; accepted 31 December 1994

## Abstract

Transport properties of solid-electrolyte layers (SEL) formed in lithium-iodine batteries have been studied by the method of single galvanostatic pulses. It was found that the rate of the anodic process depends on the formation of the ionic space charge of lithium cations injected into SEL. The values of the concentration of lithium ions and their mobility in SEL have been determined at different stages of discharge.

*Keywords:* Batteries; Lithium; Iodine; Solid-electrolyte layers

## 1. Introduction

In solid-phase lithium-iodine batteries, complexes of iodine with poly(2-vinylpyridine) (P2VP) or some other polymers are commonly used as the cathode, and lithium metal as the anode materials [1,2]. When the cathode is brought into direct contact with the anode, a solid-electrolyte layer (SEL) is formed, acting simultaneously as a separator [1]. The basic component of the SEL is lithium iodide conducted by lithium cations. During the discharge of the battery, transport of lithium ions through the SEL occurs towards the  $\text{LiI}/\text{I}_2$  (P2VP) interface where new amounts of  $\text{LiI}$  are being formed, and thus the SEL is growing in thickness [1,2]. As the SEL covering the lithium electrode has a relatively low ionic conductivity, the electrical characteristics of the lithium-iodine battery are, in general, essentially dependent on the SEL properties [2-5].

## 2. Experimental

To investigate the electrical properties of SELs in lithium-iodine batteries, the method of single galvanostatic pulses was applied. Hermetically sealed two-electrode cells with a calculated capacity of about 60 mAh were used. Along with the cathodic material based on iodine and P2VP (20 parts iodine per part P2VP by weight), the cathodic material based on iodine and

polyethylene (PE) was used (25 parts iodine per part PE by weight). In some cases,  $\text{CaO}$  powder was added to the cathodic material. The electrode surface was  $1.54 \text{ cm}^2$ . The cathode was prepared in a tablet form by pressing the cathodic material into a polytetrafluoroethylene sheet; together with an anode made from lithium metal it was placed in a stainless-steel shell and hermetically sealed. All operations were carried out in an atmosphere of dry argon. The capacity of the cells was limited by the cathode. All measurements were performed at 298 K.

Current-voltage characteristics were commonly measured after discharging the cells during different periods of time with a constant load of  $27 \text{ k}\Omega$  (prior to measurements, the cells were kept under open-circuit conditions for 1 h). In our experiments, deep discharge of a cell corresponding to the end of its service life was not attained (in this case, polarization of the cathode would make the major contribution to the overall polarization of the cell [4]). Measurements of the current-voltage characteristics were performed in both forward and backward directions (i.e. towards increasing and decreasing currents and potentials) in order to ensure that the state of the cell did not change essentially within the time of the measurements. After having obtained the current-voltage characteristics, if otherwise not stated, the cell was again connected on to a load.

For obtaining current-voltage characteristics, a ПИ-50-1 pulse potentiostat was used. The determination of the ohmic resistance and differential capacity of the cells was performed with a Г5-56 generator of rectan-

\* Corresponding author.

gular pulses. In this case, pulses of voltage were transformed to current pulses by connecting an active resistance in series in the polarization circuit, the value of which exceeded the resistance of the cell by many folds. The potential response was registered using a C8-13 memory oscilloscope.

### 3. Results and discussion

Typical potential–time oscillograms, obtained on applying current pulses to a cell in the region of low time periods and polarizations at different states of cell discharge, are shown in Fig. 1. Just after current switching, an inertialess potential leap is observed on the chronopotentiograms corresponding to the  $R_c$  resistance. Measurements of  $R_c$  were conducted for a series of lithium–iodine batteries differing in cathode thickness. The dependence of  $R_c$  on the cathode thickness obtained is satisfactorily approximated by a straight line emerging from the origin of coordinates that allow us to refer to the  $R_c$  parameter as the volume resistance of the cathode [6].

After the inertialess leap (see Fig. 1), an almost linear growth of polarization versus time is observed. From the slope of a line tangent to the initial part of the switching curve, the value of differential capacity was determined which decreased in the course of the battery discharging. The values measured remained at least by two orders of magnitude lower than those of the capacity of the double electric layer characteristics of the metal–solid electrolyte interface [7]. This allows one to assume that the differential capacity measured coincides with the geometrical capacity of the cell, i.e. with that of the capacitor in which the anode and cathode of the cell serve as the capacitor plates and the SEL as the dielectric. Taking into account that the geometrical capacity of an SEL is essentially lower than

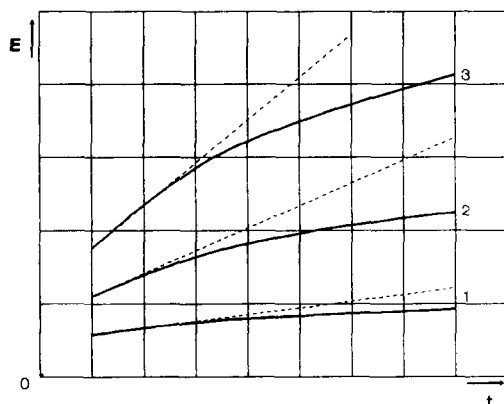


Fig. 1. Initial parts of galvanostatic switching oscillograms for various states of discharge. Cell:  $\text{Li}/\text{I}_2$  (P2VP); current:  $0.5 \mu\text{A}$ ; scale: 1 mV per scale unit,  $1 \mu\text{s}$  per scale unit. (1) 2.7 mAh; (2) 8.4 mAh, and (3) 19.2 mAh.

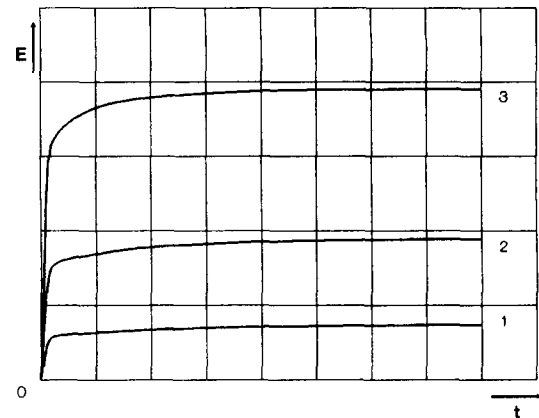


Fig. 2. Typical galvanostatic switching oscillograms for various states of discharge. Cell:  $\text{Li}/\text{I}_2$  (P2VP); current:  $4 \mu\text{A}$ ; scale: 20 mV per scale unit, 1 ms per scale unit. (1) 2.7 mAh; (2) 8.4 mAh, and (3) 19.2 mAh.

the capacities of the interfaces  $\text{Li}/\text{SEL}$  and  $\text{SEL}/\text{I}_2$  connected in series to it, their contribution to the measured capacity may be neglected. Using the geometrical capacity values measured and the formula of a parallel-plate capacitor, the effective SEL thickness values were calculated at different states of discharge of the cell. (In these calculations, the value of the SEL dielectric constant was taken to be equal to 18.2 [8].)

In Fig. 2, typical potential–time oscillograms are shown in the region of time periods sufficient for a quasi-stationary potential to be settled. Stabilized potential values were registered after switching on current pulses of different amplitudes. The values obtained, taking into account the corrections for the potential ohmic drop in the bulk of the cathode, were used for obtaining the current–voltage characteristics of the cell in a wide range of currents and potentials. The period in which a quasi-stationary value of potential was settled in the current range studied did not exceed 10 to 20 ms, therefore the quantity of electricity passing through the cell during measurements did not cause any noticeable changes in the SEL thickness and its properties.

Fig. 3(a) and (b) depicts the current–voltage characteristics of cells with cathodic materials based on iodine and P2VP, as well as on iodine and PE, respectively, obtained at different states of discharge. As can be seen from Fig. 3, the polarization dependences in the region of small currents and polarizations are straight lines emerging from the origin of coordinates, their slope increasing in the course of discharge of the cell. The values of effective ionic resistance  $R_i$ , determined from the slope of the initial part of the current–voltage characteristics, as well as of the ohmic resistance  $R_c$  found from the inertialess leaps of potential on the switching curves, for different states of cell discharge, are presented in Fig. 4. As is seen from Fig. 4, discharge of a cell leading to an increase in the amount of  $\text{LiI}$ , or to an increase in the SEL thickness,

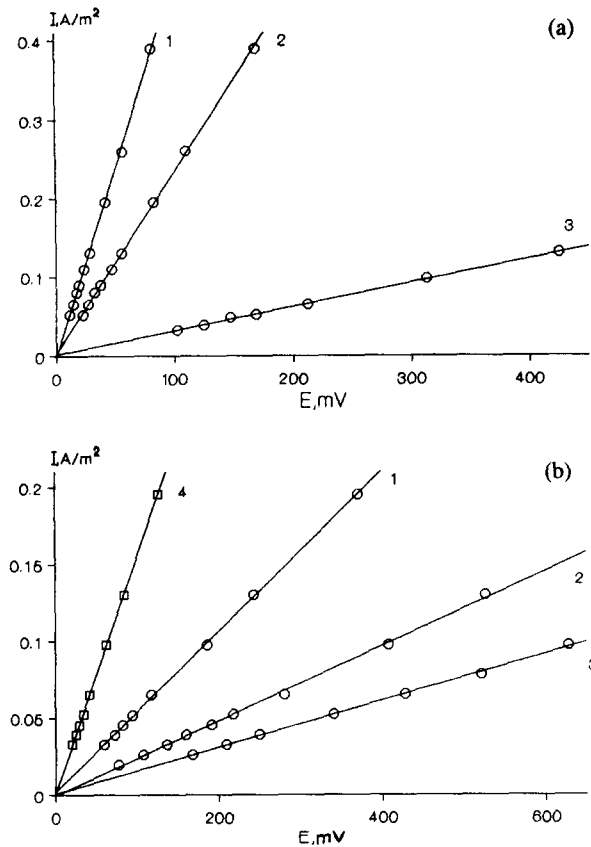


Fig. 3. Initial parts of current-voltage characteristics for various states of discharge. (a) Cell:  $Li/I_2$  (P2VP); (1) 0.4 mAh, (2) 2.7 mAh, and (3) 25.6 mAh. (b) Cell:  $Li/I_2$  (PE); (1) 0.4 mAh, (2) 2.8 mAh, (3) 9.2 mAh, and (4) cell  $Li/I_2$  (PE+CaO) 0.3 mAh.

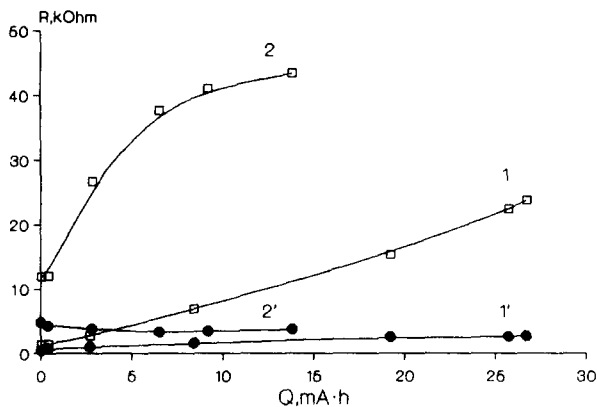


Fig. 4. (□) Ionic and (●) ohmic resistances vs. state of discharge for cells  $Li/I_2$  (P2VP) (curves (1) and (1')) and  $Li/I_2$  (PE) (curves (2) and (2')).

results in an increase of  $R_i$ . Along with that, the  $R_c$  values varies only slightly. This is in agreement with the different characters of the electrolyte- and cathode-related impedance components of the lithium-iodine batteries on discharge capacity that was observed in Ref. [4]. The dependences presented confirm the possibility of referring  $R_i$  to the process of lithium-ion

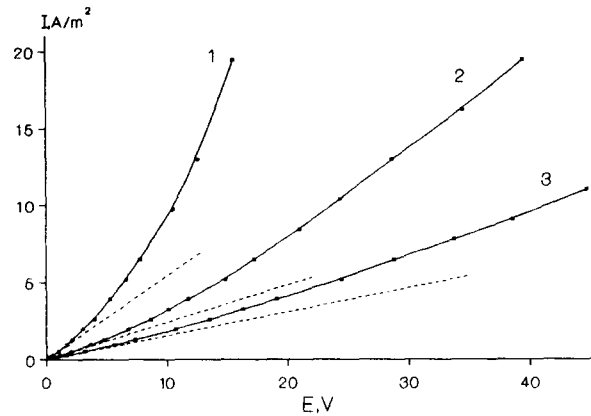


Fig. 5. Current-voltage characteristics in a wide range of current densities and polarizations. Cell:  $Li/I_2$  (PE); (1) 0.4 mAh, (2) 2.8 mAh, and (3) 9.2 mAh.

transport within the SEL bulk, and  $R_c$  to the volume resistance of the cathode.

In Fig. 5, current-voltage characteristics are shown in a wide range of current densities and polarizations. Dashed lines correspond to the initial straight current-voltage characteristic parts extrapolated to the region of high currents and polarizations. It was stated that, as the polarization increases, the current-voltage characteristics declined from the linear dependences towards increasing currents.  $I_{diff}$  is the difference between the measured value of the current ( $I_{comm}$ ) and that obtained by extrapolating the initial parts to the region of high polarization ( $I_{lin}$ ). Dependences of  $I_{diff}$  on polarization in full logarithmic coordinates for different states of discharge are presented in Fig. 6(a) and 6(b) for cells with cathodic materials based on iodine and P2VP, as well as on iodine and PE, respectively. At sufficiently high potentials, the experimental dependences  $\log I_{diff}$ ,  $\log E$  are satisfactorily approximated by straight lines with the slope equal to 2, i.e.  $I_{diff}$  is proportional to the square of polarization.

The transition from the linear current-potential dependence to a sum of linear and square dependences found for increasing polarizations shows the possibility of describing the current-voltage characteristic of the system under study within the framework of the model of space-charge-limited currents, taking into account the contribution of intrinsic current carriers [9]. In the model [10,11] used for describing the ionic transport in passivating layers on lithium in non-aqueous solutions, it is assumed that the injection of one type of carriers (lithium cations) into the SEL leads to a deterioration in electroneutrality and to a limitation of the flowing current by the resulting bulk charge. In this case, injecting lithium electrode is regarded to be an infinite reservoir of ions (ionic emitter). The condition for the appearance of a space charge is a sufficiently high value of the Maxwell's time constant (dielectric relaxation time) for the material of the SEL. As a result of that,

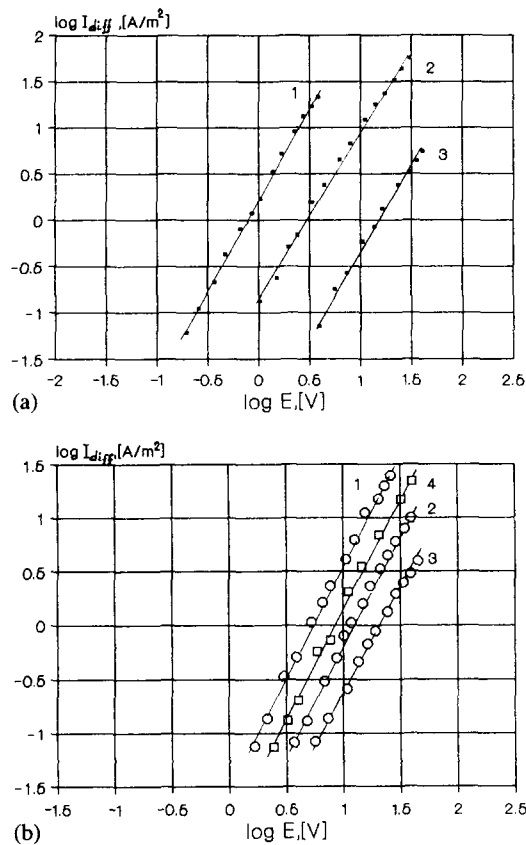


Fig. 6.  $j_{diff}$  vs.  $E$  for various states of discharge. (a) Cell:  $Li/I_2$  (P2VP); (1) 0.4 mAh, (2) 2.7 mAh, (3) 25.6 mAh. (b) Cell:  $Li/I_2$  (PE); (1) 0.4 mAh, (2) 2.8 mAh, and (3) 9.2 mAh, and (4) cell  $Li/I_2$  (PE + CaO) 0.3 mAh.

the charge of the injected carriers would have insufficient time to dissipate through the movement of the intrinsic mobile lithium ions of the SEL.

No noticeable deviations of the polarization curves from the Ohm's law appear if the average concentration of the injected lithium ions in the SEL is low as compared with that of the intrinsic mobile carriers. The transition from the Ohm's law to the square law corresponding to a mere space-charge-limited currents occurs at a potential when the charges of intrinsic mobile ions and injected cations are equal.

To describe the ionic transport through an SEL in a broad range of polarizations, the following equation [10,11] may be used:

$$I = q\mu n_0 \frac{E}{L} + \Psi(E) \epsilon\epsilon_0\mu \frac{E^2}{L^3} \quad (1)$$

which contains the concentration of intrinsic mobile lithium ions ( $n_0$ ) and their mobility ( $\mu$ ) as the parameters. Here,  $q$  is the charge of ionic current carriers,  $E$  the electrode polarization,  $L$  the SEL thickness,  $\epsilon\epsilon_0$  is the dielectric constant, and  $\Psi(E)$  a coefficient weakly dependent on the potential, of which an approximation is given in Ref. [10].

Using Eq. (1), the parameters  $n_0$  and  $\mu$ , which determine the specific ionic conductivity ( $\sigma$ ) value, were calculated from the experimental current-voltage characteristics. The behaviour of the transport parameters during discharging of the cell is represented in Fig. 7. In the region of low states of discharge, an increase in specific ionic conductivity is observed connected with a considerable growth of mobility which predominates over a decreasing concentration.

The dependences of transport parameters on the state of discharge for cells with the cathodic material based on iodine and PE are of a qualitatively similar character (see Fig. 8). In Fig. 8, two sets of curves are presented for cells differing in the addition of calcium oxide in a finely dispersed form to the cathodic material. As is seen from this Figure, the introduction of this additive leads to some decrease in the mobility and an increase in the concentration of lithium ions in the SEL. As a result, for SELs formed in cells with the cathodic material containing the above additive, the specific ionic conductivity increases by a factor of 1.5

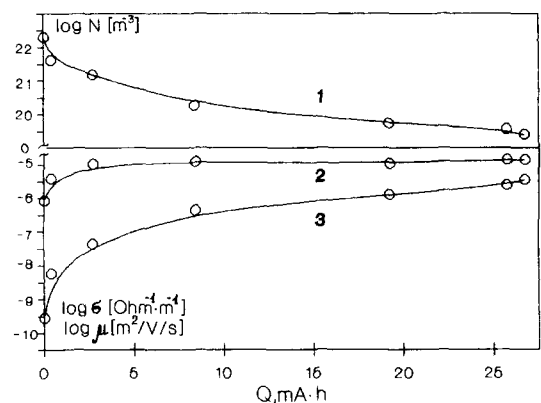


Fig. 7. Change of transport parameters during discharging of a  $Li/I_2$  (P2VP) cell: (1) concentration of mobile lithium ions in SEL, (2) specific ionic conductivity of SEL, and (3) mobility of lithium ions in SEL.

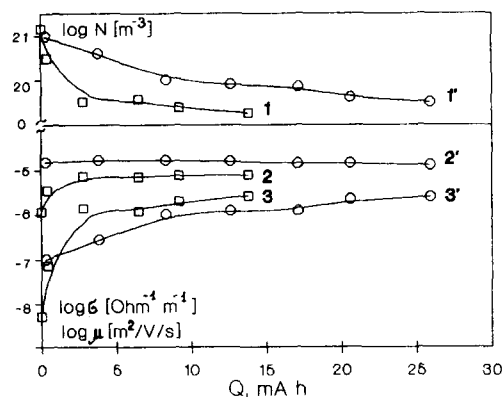


Fig. 8. Change of transport parameters during discharging of a  $Li/I_2$  (PE) cell: (1) concentration of mobile lithium ions in SEL; (2) specific ionic conductivity of SEL; (3) mobility of lithium ions in SEL; (1'), (2'), and (3') the same for a  $Li/I_2$  (PE + CaO) cell.

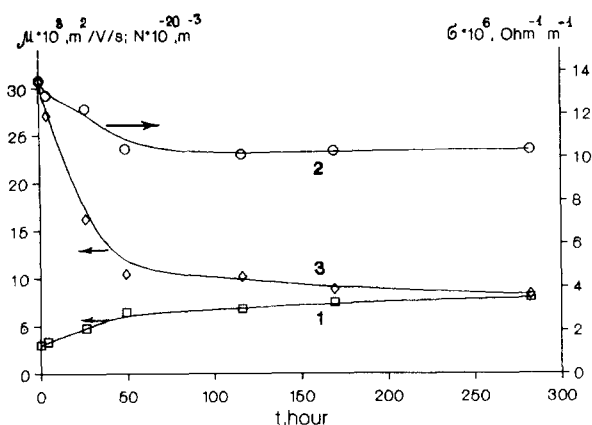


Fig. 9. Transport characteristics of SEL vs. time after discharge of an  $\text{Li}/\text{I}_2$  (P2VP) cell: (1) concentration of mobile lithium ions in SEL; (2) specific ionic conductivity of SEL, and (3) mobility of lithium ions in SEL.

to 2. Note that the specific ionic conductivity of SELs in cells with the additive practically does not change in the course of discharging, which provides evidence for the formation of SELs with the same properties at different states of discharging.

The data presented above were obtained from current–voltage characteristics registered 1 h after disconnecting the load. Special experiments were carried out to investigate the behaviour of the transport parameters of the SEL with time after disconnecting the load. The cells were discharged in an interrupted regime: after a partial discharging corresponding to the capacity value of 2 to 4 mAh, the cell was kept under open-circuit conditions. As can be seen from Fig. 9, during storage the transport parameters of the SEL change with time and then reach stationary values. Note that the observed decrease in the specific ionic conductivity value is determined basically by a relatively large drop of the mobility of lithium ions. Thus, after the complete discharging of a cell, the relaxation effect of the SEL transport properties takes place.

#### 4. Conclusions

SELs formed between the lithium electrode and an iodine-containing cathode play a determining role in the electrochemical behaviour of lithium–iodine batteries. The method used may be applied to a non-destructive determination of the electric parameters of SELs during storage and discharge of lithium–iodine batteries.

The current–voltage characteristics obtained are well described within the framework of the model of ionic space-charge-limited currents taking into account the contribution of intrinsic current carriers. Using experimental current–voltage characteristics, the main characteristics of the SEL have been determined: the con-

centration of intrinsic mobile lithium ions and their mobility, as well as the specific ionic conductivity. The parameters found fully characterize the SEL from the viewpoint of ionic transport and have not earlier been determined for these systems. The dependences of transport parameters on the state of discharge found are qualitatively similar for cells with different compositions of the cathodic material. It should be noted that the values of transport parameters found were averaged by the SEL thickness.

SELs forming in lithium–iodine batteries are well-known to be heterogeneous polycrystalline systems [5]. In particular, particles of iodinated polymer from the cathode may be included in the bulk of the SEL forming in the course of discharge of lithium–iodine batteries [5]. This accounts for the essentially higher values of specific ionic conductivity of SELs found as compared with this characteristic of single-crystal lithium iodide with point defects [12,13]. Improvement of the SEL transport properties observed after the introduction of calcium oxides in a finely dispersed form to the cathodic material (see Fig. 8) is in concordance with the known literature data [14] on the increasing conductivity of solid electrolytes upon introducing of powdered inert substances. In general, the data obtained allow us to assume that in the SEL conductivity, an important role is played by ionic transport along the intergrain boundaries.

The effect of relaxation of transport characteristics on the freshly formed SELs (see Fig. 9) may be explained within the framework of the same concept. During the discharging of a cell, a nonequilibrium polycrystalline SEL is formed which includes cathodic material particles. In the course of storage of the system, modification of  $\text{LiI}$  by cathodic material components occurs leading to alterations of its morphology and transport characteristics.

#### References

- [1] T.R. Crompton, *Small Batteries, Vol. 2, Primary Cells*, Macmillan London, 1982.
- [2] C.F. Holmes, in B.B. Owens (ed.), *Batteries for Implantable Biomedical Devices*, Plenum, New York, 1986, pp. 133–180.
- [3] A.M. Hermann and E. Luksha, in B.B. Owens and N. Margalit (eds.), *Proc. Symp. Power Sources for Biomedical Implantable Applications and Ambient Temperature Lithium Batteries*, Battery Division, the Electrochemical Society, Princeton, NJ, USA, 1980, pp. 110–121.
- [4] P.M. Skarstad and C.L. Schmidt, *Ext. Abstr., 6th Int. Meet. on Lithium batteries. Münster, Germany, 10–15 May 1992*, pp. 56–59.
- [5] R.G. Kelly and P.J. Morgan, *J. Electrochem. Soc.*, 134 (1987) 25–36.
- [6] E.S. Nimon, A.V. Shirokov, N.P. Kovynev and A.L. Lvov, *Elektrokhimiya*, 31 (1995) N4 (in Russian).
- [7] D.O. Raleigh, in M. Kleitz and J. Dupuy (eds.), *Electrode Processes in Solid State Ionics*, Riedel, Dordecht, 1976, pp. 119–144.

- [8] E.A. Ukshe and N.S. Tkachyova, *N 3095-B88*, VINITI, Moscow, 1988, (in Russian).
- [9] M.A. Lampert and P. Mark, *Injection Currents in Solids*, Academic Press, New York, 1970.
- [10] E.S. Nimon, A.V. Churikov, A.V. Shirokov, A.L. Lvov and A.N. Chuvashkin, *J. Power Sources*, 43/44 (1993) 365–375.
- [11] E.S. Nimon, A.V. Churikov, A.A. Senotov and A.L. Lvov, *Dokl. Akad. Nauk SSSR*, 303 (1988) 1180–1184 (in Russian).
- [12] J. Haven, *Recl. Trav. Chim. Pays-Bas Belg.*, 69 (1950) 1471.
- [13] B.J.H. Jackson and D.A. Young, *J. Phys. Chem. Solids*, 30 (1969) 1973–1976.
- [14] J. Maier, *J. Electrochem. Soc.*, 134 (1987) 1524–1535.